

Communication

# Inline NMR Detection of $\text{Li}^+$ in Aqueous Solutions Using a Cryogen-Free Magnet at 4.7 T

Eric Schmid <sup>1</sup>, Jens Häniisch <sup>2</sup> , Frank Hornung <sup>2</sup>, Hermann Nirschl <sup>1</sup> and Gisela Guthausen <sup>1,3,\*</sup> 

<sup>1</sup> Institute of Mechanical Process Engineering and Mechanics, Karlsruhe Institute of Technology, 76131 Karlsruhe, Germany

<sup>2</sup> Institute for Technical Physics, Karlsruhe Institute of Technology, 76344 Eggenstein-Leopoldshafen, Germany

<sup>3</sup> Chair of Water Chemistry and Water Technology, Engler-Bunte-Institut, Karlsruhe Institute of Technology, 76131 Karlsruhe, Germany

\* Correspondence: gisela.guthausen@kit.edu

## Abstract

Lithium is of major importance for many areas of technology, especially batteries, and is therefore relevant to both the industrial and private sectors. High-performance, ideally inline-compatible analytics are important for economical and environmentally friendly lithium extraction. Nuclear Magnetic Resonance is an established analytical method that has already been used in numerous inline applications. For this study on  ${}^7\text{Li}$  NMR in flow, a cryogen-free magnet with a variable magnetic field was used, whereby a field strength of 4.7 T was set for the measurements for compatibility reasons. The influences of flow velocity, repetition time, and lithium concentration were investigated in spin echo measurements. This allows for defining limitations and potential fields of application for the measurement setup. In addition, the possibilities of internal pre-polarization were investigated. The results show that the method and setup are well suited for inline flow measurements on  ${}^7\text{Li}$  and have great potential for expanding the range of applications.

**Keywords:** NMR; inline process monitoring; lithium extraction; relaxation; lithium NMR; cryogen-free magnet; mobile NMR

## 1. Introduction

Lithium has become an incredibly important raw material for numerous technologies, particularly for the production of high-performance batteries for electric mobility and mobile electronic devices [1]. The limited resources that can currently be economically exploited via mining make the development of new technologies and the exploitation of further mining areas attractive from both economic and ecological perspectives. Suitable process-compatible analysis methods are essential for powerful, efficient, and sustainable technical processes for lithium extraction. Inline methods offer advantages over offline methods in that chemical or physical measurements are available almost instantly while being non-destructive and contactless, thereby providing the basis for an efficient and agile technical process [2]. This increases lithium output and reduces energy consumption on the one hand. On the other hand, since the salt solutions are corrosive, this approach of minimum sample preparation and treatment in a closed loop leads to minimum destruction of the measurement equipment.

Nuclear Magnetic Resonance (NMR) is a widely used and well-established analytical tool with applications both in research, such as chemical structure elucidation, and in the industrial sector, for example, in quality control [3–8]. Industrial NMR applications



Academic Editor: Igor Serša

Received: 17 December 2025

Revised: 7 January 2026

Accepted: 9 January 2026

Published: 13 January 2026

**Copyright:** © 2026 by the authors.

Licensee MDPI, Basel, Switzerland.

This article is an open access article distributed under the terms and conditions of the [Creative Commons](#)

[Attribution \(CC BY\) license](#).

require monitoring tools that are robust against external influences in a process plant, generate a small magnetic stray field, and are easy to operate with low maintenance needs. Classic high-field NMR instruments with their superconducting magnets cooled with liquid helium and nitrogen are often unsuitable for this purpose. Furthermore, mobile applications are hardly feasible. Instead, low-field NMR with permanent magnets is well suited for this purpose and has already been used extensively for inline applications [9–15]. A low-field NMR sensor for  $^{7}\text{Li}$  inline measurements on lithium-containing brines has also been developed and applied [16]. However, when measuring nuclei other than  $^{1}\text{H}$  and samples with small concentrations of the target product, a stronger magnetic field  $B_0$  should be used to increase the signal-to-noise ratio. The gyromagnetic ratio  $\gamma$  of  $^{7}\text{Li}$  is a factor of 2.573 smaller than that of  $^{1}\text{H}$ , the spin quantum number is 3/2, and the natural abundance is with 92.4% slightly lower than of  $^{1}\text{H}$  so that a stronger  $B_0$  with inherently larger sensitivity is desirable for the development of process-compatible applications of  $^{7}\text{Li}$  NMR [17–19].

In this study,  $^{7}\text{Li}$  NMR on flowing aqueous lithium chloride (LiCl) solutions was performed with a superconducting, cryogen-free magnet at a  $B_0$  of 4.7 T as a basis for the development of an inline-capable measurement method for monitoring the lithium concentration in process streams during lithium extraction. In addition to the influence of lithium concentration, the influences of flow velocity, repetition time, and polarization length were also investigated. A compact, industrial-grade Bruker minispec NF instrument was used as electronic unit in order to realize a potentially mobile and space-saving setup.

## 2. Results and Discussion

The maximum signal intensities  $I_{\max}$  of the Hahn echo envelopes are plotted as a function of the mean velocity to show the dependencies on the respective parameters. A value of 100% corresponds to the maximum signal intensity that can be correctly processed by the receiver. For the solution with  $c_{\text{LiCl}} = 27.1 \text{ g/L}$  and  $l_{\text{pol}} = 30 \text{ cm}$ ,  $I_{\max}$  decreases with increasing  $v_{\text{mean}}$  (Figure 1, red data points). However, for sufficiently small  $v_{\text{mean}}$ ,  $I_{\max}$  increases compared to the static case of  $v_{\text{mean}} = 0 \text{ cm/s}$ . This can be explained by the inflow effect, which is well known in flow NMR [20,21]: The flow causes fresh, polarized, but unexcited spins to flow into the sensitive area after previous excitation and echo detection during the repetition time. In the next experiment, their magnetization can be excited, thereby reducing integral saturation effects. This results in a larger integral signal intensity if the repetition time  $RD$  is smaller than five times the longitudinal relaxation time  $T_1$ . For larger  $v_{\text{mean}}$ , the residence time in the static magnetic field  $B_0$  along the polarization length of 0.3 m is not sufficient for an almost complete polarization due to the long  $T_1$  of  $^{7}\text{Li}$  of around 8 s [16]. This results in smaller  $I_{\max}$  values. Please note that  $RD = 15 \text{ s}$  in Figure 1 already results in partial saturation in non-flowing liquids and, thus, smaller  $I_{\max}$ . For static measurements,  $RD$  would have to be significantly larger.

The measurements show that the selected experimental setup with the cryogen-free magnet can be used for measurements on  $^{7}\text{Li}$ , even in flow. The impact of the flow velocity can clearly be derived from the signal intensity as a consequence of the inflow effect, even at the small pre-polarization length. The investigation of the influence of the internal pre-polarization length on the measurement results additionally provides a basis for further potential applications of the magnet. The large bore allows the tube to be wound up in the magnet, increasing  $l_{\text{pol}}$  here to 120 cm.

The signal intensities are larger for the longer pre-polarization length  $l_{\text{pol}} = 1.2 \text{ m}$  (Figure 1, black data points), which is explained by the larger residence time and the more pronounced longitudinal magnetization build-up. However, the influence of the inflow effect can still be observed. A further increase in the internal  $l_{\text{pol}}$  will result in a larger signal

intensity, making the magnet well suited for experiments with the need for pre-polarization, which is especially the case for moieties with long  $T_1$  and low NMR sensitivity.

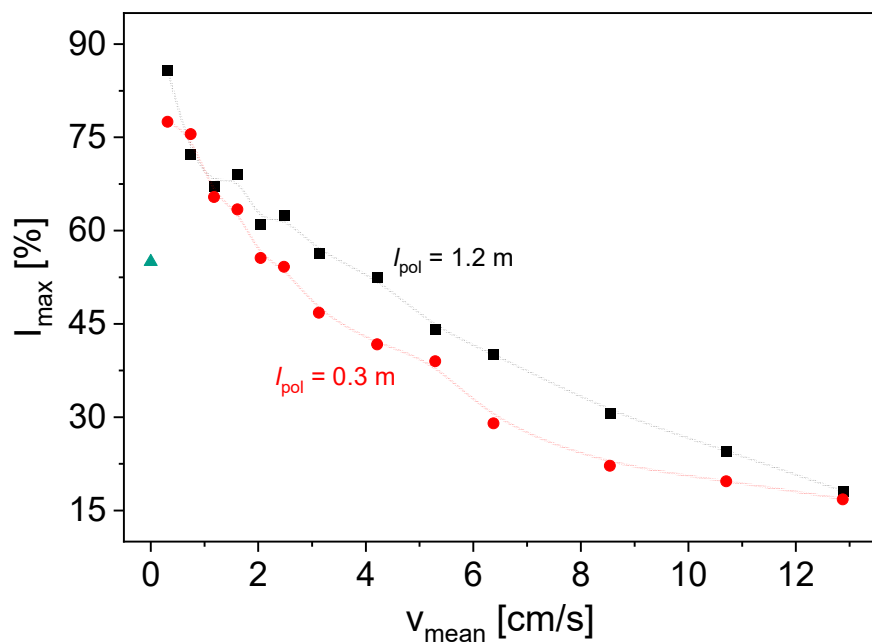


**Figure 1.**  $I_{\text{max}}$  as a function of  $v_{\text{mean}}$  for a LiCl solution with  $c_{\text{LiCl}} = 27.1 \text{ g/L}$  and  $RD = 15 \text{ s}$ , with  $l_{\text{pol}} = 0.3 \text{ m}$  (●) and  $l_{\text{pol}} = 1.2 \text{ m}$  (■). The longer pre-polarization length leads to a larger signal intensity, whereby the dependence of  $I_{\text{max}}$  on  $v_{\text{mean}}$  is roughly the same for both  $l_{\text{pol}}$ . B-Splines are guides for the eye.  $I_{\text{max}}$  for  $v_{\text{mean}} = 0 \text{ cm/s}$  is displayed as ▲.

In addition to  $v_{\text{mean}}$ , the repetition time  $RD$  was varied (Figure 2). For  $v_{\text{mean}} = 0 \text{ cm/s}$ ,  $I_{\text{max}}$  increases with increasing  $RD$ . This is due to saturation effects as a result of the large  $T_1$  of  $^7\text{Li}$  in the used sample. For  $v_{\text{mean}} > 0 \text{ cm/s}$ , the influence of  $l_{\text{pol}}$  is clearly noticeable. Larger  $l_{\text{pol}}$  leads to larger  $I_{\text{max}}$ . Furthermore, a plateau in  $I_{\text{max}}$  occurs as a function of  $RD$  for  $v_{\text{mean}} > 0 \text{ cm/s}$ , which is explained by the inflow effect and the smaller influence of saturation effects. At small  $RD$  and medium  $v_{\text{mean}}$ , an increase in  $I_{\text{max}}$  due to the inflow effect can be seen when compared to  $v_{\text{mean}} = 0 \text{ cm/s}$ . For larger velocities, the shorter residence time in  $B_0$  and smaller pre-polarization lead to reduced  $I_{\text{max}}$ . In addition, the outflow effect needs to be considered. The benefit of the described setup becomes obvious in the left part of the graph:  $I_{\text{max}}$  is considerably larger at moderate velocities, even at the largest velocity of  $10.7 \text{ cm/s}$ , and  $I_{\text{max}}$  is in the range of thermal polarization for the larger pre-polarization length. This observation allows for reducing the repetition time considerably to reasonable values: for example,  $RD$  around  $1 \text{ s}$  instead of  $8 \text{ s}$  for  $l_{\text{pol}} = 1.2 \text{ m}$  and  $v_{\text{mean}} = 6.4 \text{ cm/s}$ , which results in eight times faster experiments or a significant gain in the signal-to-noise ratio. The observations are consistent with expectations, making the experimental setup and the selected parameter ranges suitable for these applications.

The three-dimensional ( $v_{\text{mean}}$ ,  $RD$ , and  $l_{\text{pol}}$ ) parameter space was examined using full factorial design so that all inter-dependencies could be identified. The experiments with  $c_{\text{LiCl}} = 27.1 \text{ g/L}$  show a sufficiently large signal intensity for the investigation of the respective influences for all parameter combinations (Figure 3).

Spin echoes could also be detected for the aqueous solution of the smaller concentration  $c_{\text{LiCl}} = 15.6 \text{ g/L}$ . The measurement settings have been adjusted accordingly.  $I_{\text{max}}$  at  $v_{\text{mean}} > 4.2 \text{ cm/s}$  is barely distinguishable from the noise level, so these data points are not shown (Figure 4).

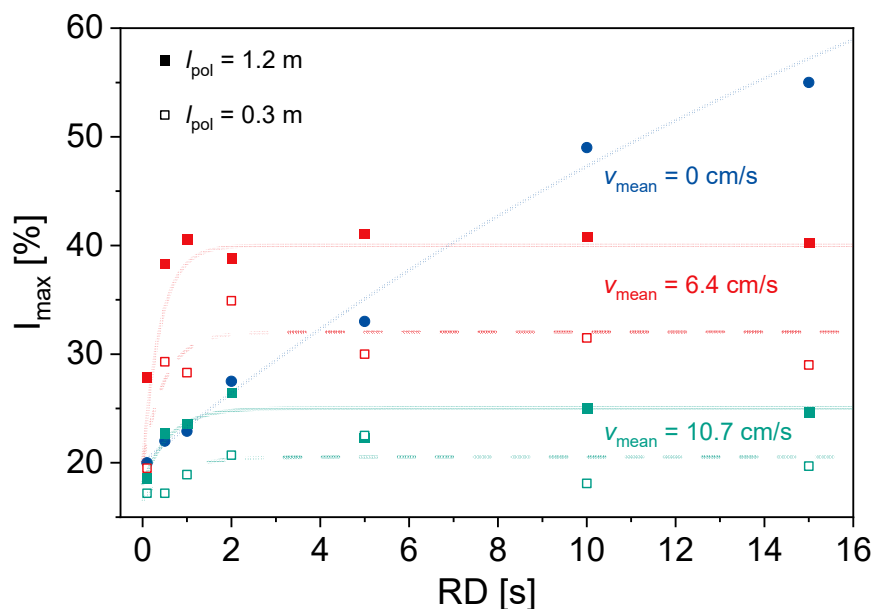


**Figure 2.**  $I_{\max}$  for  $c_{\text{LiCl}} = 27.1 \text{ g/L}$  as a function of  $RD$  for (●)  $v_{\text{mean}} = 0 \text{ cm/s}$ ; (■)  $l_{\text{pol}} = 1.2 \text{ m}$ ,  $v_{\text{mean}} = 6.4 \text{ cm/s}$ ; (□)  $l_{\text{pol}} = 0.3 \text{ m}$ ,  $v_{\text{mean}} = 6.4 \text{ cm/s}$ ; (■)  $l_{\text{pol}} = 1.2 \text{ m}$ ,  $v_{\text{mean}} = 10.7 \text{ cm/s}$ ; and (□)  $l_{\text{pol}} = 0.3 \text{ m}$ ,  $v_{\text{mean}} = 10.7 \text{ cm/s}$ . Lines are guide for the eyes.  $I_{\max}$  increases with increasing  $RD$ . A longer pre-polarization length results in a larger  $I_{\max}$ . For smaller  $RD$ ,  $I_{\max}$  for  $v = 0 \text{ cm/s}$  is between the values of  $I_{\max}$  for  $v > 0 \text{ cm/s}$ , and for larger  $RD$ ,  $I_{\max}$  for  $v = 0 \text{ cm/s}$  is the largest.

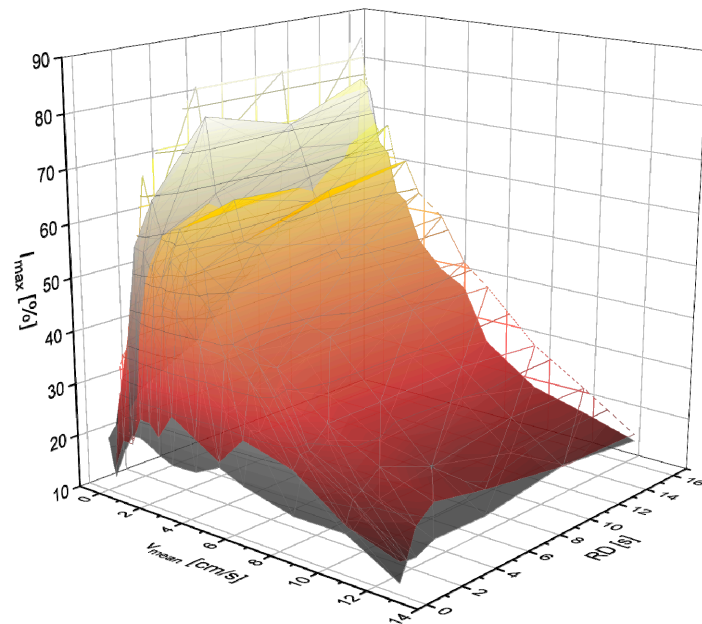


**Figure 3.**  $I_{\max}$  for  $c_{\text{LiCl}} = 27.1 \text{ g/L}$  as a function of  $v_{\text{mean}}$  and  $RD$  for a LiCl solution with  $l_{\text{pol}} = 0.3 \text{ m}$  (gray scale) and  $l_{\text{pol}} = 1.2 \text{ m}$  (yellow-red scale).

Also, at smaller concentrations, the positive influence of the longer  $l_{\text{pol}}$  on  $I_{\max}$  is clear. The experiments with smaller  $c_{\text{LiCl}}$  reveal the limitations of the current measurement setup in terms of  $\text{Li}^+$  concentration and flow velocity range.

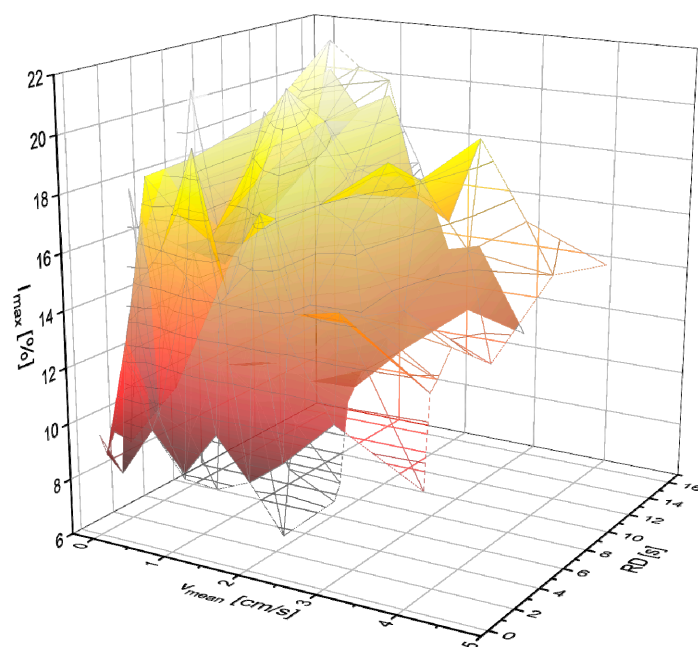


**Figure 4.**  $I_{\max}$  for  $c_{\text{LiCl}} = 15.6$  g/L as a function of  $v_{\text{mean}}$  and  $RD$  for a LiCl solution with  $l_{\text{pol}} = 0.3$  m (gray scale) and  $l_{\text{pol}} = 1.2$  m (yellow-red scale).

### 3. Materials and Methods

The superconducting magnet used for the investigations consists of a NbTi magnet coil and generates a maximum  $B_0$  of 5 T in a warm vertical bore of 180 mm diameter (Figure 5). The magnet is operated at 4 K and cooled without cryogen using a cryocooler. The cool-down process takes approximately 80 h, whereby only a power supply is required. In the cold state, the maximum field is reached within 42 min. The axial  $B_0$  homogeneity in the relevant area is <1%, and neither cryogenic nor room temperature shim systems are included. Chemical resolution is not the focus of the measurement method as only  $\text{Li}^+$  ions were observed. For compatibility reasons with results on a conventional helium-cooled NMR magnet, a  $B_0$  of 4.7 T was selected, which corresponds to a  $^7\text{Li}$  Larmor frequency of 77.81 MHz. The electronic unit of a Bruker minispec NF series (Bruker BioSpin GmbH & Co. KG, Ettlingen, Germany) was used for control, pulse generation, and data acquisition, whereby the preamplifier was modified in order to extend the frequency range. A Bruker MICWB40  $^7\text{Li}$  25 mm LTR micro imaging probe (Bruker BioSpin MRI GmbH, Ettlingen, Germany) was used for the experiments.

The Hahn echo pulse sequence was selected for the measurements [22]. In this pulse sequence, a  $90^\circ$  excitation pulse is followed by a  $180^\circ$  refocusing pulse after the half echo time  $\tau_e$  and then by the detection of a spin echo after a further delay of  $\tau_e/2$ . In contrast to single-pulse acquisition, the Hahn echo pulse sequence refocuses the dephasing due to static magnetic field inhomogeneities, making it more suitable for measurements with the magnet used. Since the transverse NMR relaxation properties of the sample were not of interest for the fundamental investigations of this work, measurements were only performed at one echo time so that no echo train was acquired. This enables fast, quantitative measurements of lithium concentration, which is necessary for potential inline applications in quality control and process management.

For the flow-through measurements and to show the principle on the lab scale, a fluidic circuit was built through the magnet. It comprised a reservoir tank, a peristaltic pump (Watson-Marlow 323 S, Watson-Marlow Ltd., Falmouth, UK), and a pressure compensation tank to reduce flow pulsation before the fluid enters the magnet (Figure 6). A tube of polyurethane with an inner diameter of 7 mm was passed through the probe. The flow

direction was selected from bottom to top, and the sample was recirculated for longer total experiment times. The probe was positioned in the magnet from the top and held in a reproducible position with a cover plate and precision spacers. A straight, i.e., shortest, possible arrangement of the tube results in a pre-polarization length  $l_{\text{pol}}$  of 30 cm from the lower edge of the magnet to the sensitive area of the probe. To realize a longer pre-polarization length, the tube was wound in a spiral and positioned in the magnet, resulting in  $l_{\text{pol}} = 120$  cm.



**Figure 5.** Picture of the magnet on a stand in the front and the NMR control units in the back.

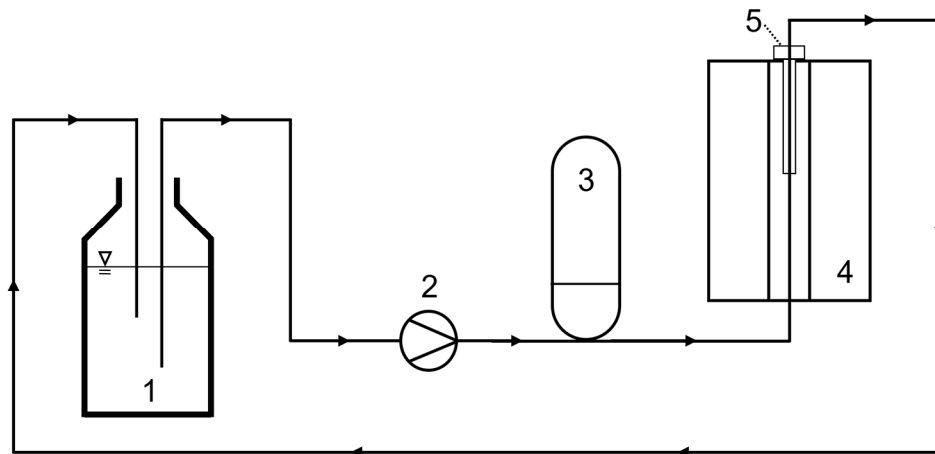


**Figure 6.** Scheme of the experimental flow setup with the reservoir (1), the peristaltic pump (2), the pressure compensation tank (3), the magnet (4), and the probe (5). The sample is recirculated back to the reservoir.

To prove the sensitivity of the measurements on  ${}^7\text{Li}$ , two aqueous LiCl (Sigma-Aldrich, St. Louis, MO, USA) solutions with concentrations of  $c_{\text{LiCl}} = 27.1$  g/L and 15.6 g/L were prepared. The solutions were mixed by adding crystalline LiCl to deionized water and shaking the vessel for several minutes. Measurements were made on both solutions in flow at different mean flow velocities  $v_{\text{mean}}$  and repetition times (relaxation delay  $RD$ ). The NMR measurement parameters were determined individually for both concentrations (Table 1).

**Table 1.** Measurement and experiment parameters of the flow measurements with the two aqueous LiCl solutions.

Parameter	$c_{\text{LiCl}} = 27.1 \text{ g/L}$	$c_{\text{LiCl}} = 15.6 \text{ g/L}$
Echo time $\tau_e$ (ms)	1.0	1.0
Repetition time $RD$ (s)	0.1 … 15	0.1 … 15
Number of averages (—)	8	16
Receiver gain (dB)	84	88
$v_{\text{mean}}$ (cm/s)	0 … 12.9	0 … 4.2
$l_{\text{pol}}$ (cm)	30; 120	30; 120

#### 4. Conclusions

The suitability of a cryogen-free magnet at 4.7 T for  $^7\text{Li}$  NMR on flowing samples, for example, in a lithium extraction plant, were investigated. The Hahn echo pulse sequence was used to measure signal intensities and thus make quantitative determinations about lithium concentration. By varying the mean flow velocity and the repetition time, information was obtained about the usability in a process plant and about the influences of the inflow effect on the NMR measurements in the desired area of application. The experiments with two different LiCl concentrations revealed corresponding limitations with regard to the LiCl concentration. The method can therefore be applied in the product streams of a production plant with sufficiently large lithium concentrations. In addition to the suitability of the cryogen-free magnet for  $^7\text{Li}$  NMR measurements, it was also shown that the magnet can be used for internal pre-polarization and that positive effects on the measurement results can be generated. Based on the investigations shown here, measurements could be made on lithium-containing solutions from a real production plant that offers, in addition, considerable paramagnetic relaxation enhancement in the natural composition for the reduction of Li measurement time. This effect could also be used to investigate the influence of other components, particularly those of these paramagnetic constituents. NMR relaxation measurements can also be considered for this purpose in order to gain in-depth insight, also in form of multiple echo sequences. Furthermore, measurements on other NMR-active nuclei and a comprehensive characterization of the pre-polarization properties are conceivable at the larger magnetic fields in comparison to permanent magnets. A further improvement in the measurement process can be achieved by further increasing the polarization length in the magnet. In addition, the sample volume can be increased to further improve the signal-to-noise ratio, which, together with multi-echo sequences, will result in the real inline NMR determination of Li ion content along the enrichment process.

**Author Contributions:** Conceptualization, E.S., J.H. and G.G.; methodology, E.S. and G.G.; validation, E.S., F.H. and G.G.; formal analysis, E.S. and G.G.; investigation, E.S. and G.G.; resources, H.N. and G.G.; data curation, E.S.; writing—original draft preparation, E.S., J.H. and G.G.; writing—review and editing, E.S., J.H., F.H., H.N. and G.G.; visualization, E.S., J.H. and G.G.; supervision, G.G.; project administration, J.H. and G.G.; funding acquisition, H.N. and G.G. All authors have read and agreed to the published version of the manuscript.

**Funding:** This study was funded by the Deutsche Forschungsgemeinschaft (DFG)—Project-ID 454252029—SFB/CRC 1527.

**Institutional Review Board Statement:** Not applicable.

**Informed Consent Statement:** Not applicable.

**Data Availability Statement:** The data are available on request from the authors.

**Acknowledgments:** The authors thank Philipp Heger and Paul Jelden (ITEP) for technical assistance and the Bruker minispec development group for the design and production of a dedicated preamplifier. The Deutsche Forschungsgemeinschaft is thanked for the substantial financial contribution in the form of NMR instrumentation within the instrumental facility Pro<sup>2</sup>NMR and within the CRC 1527 Hyperion.

**Conflicts of Interest:** The authors declare no conflicts of interest.

## Abbreviations

The following abbreviations are used in this manuscript:

LiCl	Lithium chloride
NMR	Nuclear magnetic resonance

## References

1. Steiger, K.; Hilgers, C.; Kolb, J. *Lithiumbedarf Für Die Batteriezellen-Produktion in Deutschland und Europa im Jahr 2030*; KIT: Karlsruhe, Germany, 2022.
2. Bowler, A.L.; Bakalis, S.; Watson, N.J. A review of in-line and on-line measurement techniques to monitor industrial mixing processes. *Chem. Eng. Res. Des.* **2020**, *153*, 463–495. [\[CrossRef\]](#)
3. Wüthrich, K. NMR studies of structure and function of biological macromolecules. *Biosci. Rep.* **2003**, *23*, 119–153. [\[CrossRef\]](#) [\[PubMed\]](#)
4. Chinn, S.C.; Cook-Tendulkar, A.; Maxwell, R.; Wheeler, H.; Wilson, M.; Xie, Z.H. Qualification of Automated Low-Field NMR Relaxometry for Quality Control of Polymers in a Production Setting. *Polym. Test.* **2007**, *26*, 1015–1024. [\[CrossRef\]](#)
5. Mitchell, J.; Gladden, L.F.; Chandrasekera, T.C.; Fordham, E.J. Low-field permanent magnets for industrial process and quality control. *Prog. Nucl. Magn. Reson. Spectrosc.* **2014**, *76*, 1–60. [\[CrossRef\]](#) [\[PubMed\]](#)
6. Fan, K.; Zhang, M. Recent developments in the food quality detected by non-invasive nuclear magnetic resonance technology. *Crit. Rev. Food Sci. Nutr.* **2019**, *59*, 2202–2213. [\[CrossRef\]](#) [\[PubMed\]](#)
7. Kern, S.; Wander, L.; Meyer, K.; Guhl, S.; Mukkula, A.R.G.; Holtkamp, M.; Salge, M.; Fleischer, C.; Weber, N.; King, R.; et al. Flexible automation with compact NMR spectroscopy for continuous production of pharmaceuticals. *Anal. Bioanal. Chem.* **2019**, *411*, 3037–3046. [\[CrossRef\]](#) [\[PubMed\]](#)
8. Kern, S.; Meyer, K.; Guhl, S.; Grasser, P.; Paul, A.; King, R.; Maiwald, M. Online low-field NMR spectroscopy for process control of an industrial lithiation reaction-automated data analysis. *Anal. Bioanal. Chem.* **2018**, *410*, 3349–3360. [\[CrossRef\]](#) [\[PubMed\]](#)
9. Schmid, E.; Rondeau, S.; Rudszuck, T.; Nirschl, H.; Guthausen, G. Inline NMR via a Dedicated V-Shaped Sensor. *Sensors* **2023**, *23*, 2388. [\[CrossRef\]](#) [\[PubMed\]](#)
10. Schmid, E.; Pertzel, T.O.; Nirschl, H.; Guthausen, G. Characterization of Flow with a V-Shaped NMR Sensor. *Sensors* **2024**, *24*, 6163. [\[CrossRef\]](#) [\[PubMed\]](#)
11. Herold, H.; Hardy, E.H.; Ranft, M.; Wassmer, K.H.; Nestle, N. Online Rheo-TD NMR for analysing batch polymerisation processes. *Microporous Mesoporous Mater.* **2013**, *178*, 74–78. [\[CrossRef\]](#)
12. Corver, J.; Guthausen, G.; Kamrowski, A. In-line non-contact check weighing (NCCW) with nuclear magnetic resonance (NMR) presents new opportunities and challenges in process control. *Pharm. Eng.* **2005**, *25*, 18–30.
13. Colnago, L.A.; Andrade, F.D.; Souza, A.A.; Azereedo, R.B.V.; Lima, A.A.; Cerioni, L.M.; Osan, T.M.; Pusiol, D.J. Why is Inline NMR Rarely Used as Industrial Sensor? Challenges and Opportunities. *Chem. Eng. Technol.* **2014**, *37*, 191–203. [\[CrossRef\]](#)
14. Foley, D.A.; Bez, E.; Codina, A.; Colson, K.L.; Fey, M.; Krull, R.; Piroli, D.; Zell, M.T.; Marquez, B.L. NMR flow tube for online NMR reaction monitoring. *Anal. Chem.* **2014**, *86*, 12008–12013. [\[CrossRef\]](#) [\[PubMed\]](#)
15. Keifer, P.A. Flow techniques in NMR spectroscopy. *Annu. Rep. NMR Spectrosc.* **2007**, *62*, 1–47. [\[CrossRef\]](#)
16. Schmid, E.; Lerner, R.; Rudszuck, T.; Nirschl, H.; Guthausen, G. Inline Monitoring of Lithium Brines with Low-Field NMR. *Appl. Sci.* **2025**, *15*, 9987. [\[CrossRef\]](#)
17. Fukushima, E.; Roeder, S.B.W. *Experimental Pulse NMR, A Nuts and Bolts Approach*; Addison-Wesley Publishing Company Inc.: London, UK, 1981.
18. Abragam, A. *Principles of Nuclear Magnetism*; Oxford University Press: Oxford, UK, 1961.
19. Blümich, B. *Essential NMR*; Springer: Berlin/Heidelberg, Germany, 2005.
20. Pope, J.M. Quantitative NMR Imaging of Flow. *Concept. Magn. Res.* **1993**, *5*, 281–302. [\[CrossRef\]](#)

21. Gao, J.-H.; Liu, H.-L. Inflow effects on functional MRI. *NeuroImage* **2012**, *62*, 1035–1039. [[CrossRef](#)] [[PubMed](#)]
22. Hahn, E.L. Spin Echoes. *Phys. Rev.* **1950**, *80*, 580–594. [[CrossRef](#)]

**Disclaimer/Publisher's Note:** The statements, opinions and data contained in all publications are solely those of the individual author(s) and contributor(s) and not of MDPI and/or the editor(s). MDPI and/or the editor(s) disclaim responsibility for any injury to people or property resulting from any ideas, methods, instructions or products referred to in the content.